Proc. Natl. Acad. Sci. USA
Vol. 89, pp. 11093–11097, November 1992
Cell Biology

Cytoskeletal integrity in interphase cells requires protein phosphatase activity

JOHN E. ERIKSSON*†, DAVID L. BRAUTIGAN‡, RICHARD VALLEE§, JOANNA OLMSTED¶, HIROTA FUJIKI||, AND ROBERT D. GOLDMAN*

*Department of Cell, Molecular, and Structural Biology, Northwestern University Medical School, 303 East Chicago Avenue, Chicago, IL 60611-3008; ‡Section of Biochemistry, Brown University, Providence, RI 02912; §Department of Cell Biology, Worcester Foundation for Experimental Biology, 222 Maple Avenue, Shrewsbury, MA 01545; ¶Department of Biology, University of Rochester, Rochester, NY 14627-0211; and ||Cancer Prevention Division, National Cancer Center Research Institute, Tsukiji 5-chome, Chuo-ku, Tokyo, Japan

Communicated by Eric H. Davidson, August 3, 1992 (received for review March 5, 1992)

ABSTRACT **Phosphorylation by protein kinases has been established as a key factor in the regulation of cytoskeletal structure. However, little is known about the role of protein phosphatases in cytoskeletal regulation. To assess the possible functions of protein phosphatases in this respect, we studied the effects of the phosphatase inhibitors calyculin A, okadaic acid, and dinophysistoxin 1 (35-methylokadaic acid) on BHK-21 fibroblasts. Within minutes of incubation with these inhibitors, changes are seen in the structural organization of intermediate filaments, followed by a loss of microtubules, as assayed by immunofluorescence. These changes in cytoskeletal structure are accompanied by a rapid and selective increase in vimentin phosphorylation on interphase-specific sites, and they are fully reversible after removal of calyculin A. The results indicate that there is a rapid phosphate turnover on cytoskeletal intermediate filaments and further suggest that protein phosphatases are essential for the maintenance and structural integrity of two major cytoskeletal components.**

Phosphorylation is involved in the regulation of all major cytoskeletal components. It has been shown that phosphorylation is a principal factor in the regulation of intermediate filament (IF) polymerization, subcellular organization, and dynamics (1, 2). IF proteins are substrates for several different kinases, including $p34^{cdc2}$ kinase (1, 2). In the latter case, hyperphosphorylation of vimentin-containing IF is directly correlated with their disassembly into protofilamentous structures (3–5). It has also been suggested that microtubules (MTs) and MT-associated proteins (MAPs) are affected by phosphorylation (6–9). Furthermore, actomyosin complexes are also regulated by phosphorylation of either actin-associated proteins, such as caldesmon (10), or the heavy and light chains of myosin (11). Studies on the regulation of cytoskeletal structure and function by phosphorylation have thus far focused on the roles of different kinases. In contrast, little attention has been given to the role of protein phosphatases, although there are some studies indicating that they may be important in the regulation of the actomyosin system (12–14). In this study we attempted to describe the role of protein phosphatases in the regulation of IFs and MTs in BHK-21 cells. To this end, we have employed the phosphatase inhibitors okadaic acid (OA), dinophysistoxin 1 (35-methylokadaic acid; DT), and calyculin A (cl-A). These three substances are potent and specific inhibitors of the type 1 (PP1) and type 2A (PP2A) serine/threonine phosphatases (15). However, although cl-A, DT, and OA inhibit PP2A with similar potency, cl-A is 50- to 100-fold more effective as a PP1 inhibitor (15).

The publication costs of this article were defrayed in part by page charge payment. This article must therefore be hereby marked "*advertisement*" in accordance with 18 U.S.C. §1734 solely to indicate this fact.

MATERIALS AND METHODS

Cell Culture and Immunofluorescence. BHK-21 cells, grown on 22-mm^2 glass overslips as described (16), were processed for double-label indirect immunofluorescence as described (16, 17). The rabbit polyclonal vimentin (17) and mouse monoclonal β-tubulin (N-357, Amersham) antibodies were visualized by the secondary antibodies fluorescein-conjugated goat anti-rabbit IgG and rhodamine-conjugated goat anti-mouse IgG (Kirkegaard and Perry Laboratories, Gaithersburg, MD), respectively. Staining of filamentous actin with rhodamine-phalloidin (Molecular Probes) was carried out as described (18).

Identification of Phosphoproteins. Phosphoproteins were studied either by immunoprecipitation or by identification of ^{32}P-labeled protein bands on Western blots. Subconfluent cell cultures were preincubated for 1.5–12 h at 37°C in culture medium containing [^{32}P]orthophosphate (150 μCi/ml; 1 Ci = 37 GBq), before phosphatase inhibitors were added. The length of preincubation did not affect the results. After incubation, cells were washed with phosphate-buffered saline and lysed in 0.4% SDS/20 mM Tris·HCl, pH 7.2/5 mM EGTA/5 mM EDTA/10 mM sodium pyrophosphate, and the lysates were heated at 100°C for 10 min (5). The phosphatase inhibitors cl-A, OA, and DT were isolated as described (19), without any traces of halichondrin in the inhibitor preparations (H.F., unpublished observations). Immunoprecipitation of vimentin (17), the IF-associated protein IFAP-300K (16), MAP-4 (20), and tubulin (21) was carried out as described (4, 5), using polyclonal rabbit antibodies and protein A-Sepharose (Sigma). Immunoprecipitation of MAP-1A (22) and MAP-1B (23) was carried out by using mouse monoclonal antibodies and anti-mouse IgG antibodies conjugated to agarose beads (Sigma) as described (23). The ^{32}P-labeled immunoprecipitated proteins were then separated on SDS/7.5% polyacrylamide gels (SDS/PAGE; ref. 24). Gels were dried and autoradiographed at −70°C using Kodak X-Omat AR film. ^{32}P labeling was determined from scans of the autoradiographs by using an LKB UltroScan densitometer (Pharmacia) or the Fujix BAS 2000 bioimaging analyzer (Fuji).

In vivo ^{32}P labeling of myosin heavy and light chains was measured from autoradiographs of Western blots of whole cell lysates. These proteins were detected with a polyclonal antibody against myosin heavy chain (21) and a mouse monoclonal antibody against myosin light chain (M4401, Sigma).

Two-Dimensional ^{32}P-Labeled Peptide Mapping. Cells were preincubated for 3 h with [^{32}P]orthophosphate (300 μCi/ml) in phosphate-free DMEM supplemented with 10% (vol/vol) calf serum (3), before addition of cl-A. To minimize labeling

Abbreviations: cl-A, calyculin A; OA, okadaic acid; DT, dinophysistoxin 1; IF, intermediate filament; MT, microtubule; MAP, MT-associated protein; PP1 and PP2A, protein phosphatase types 1 and 2A, respectively; AU, absorbance unit(s).

†To whom reprint requests should be addressed.

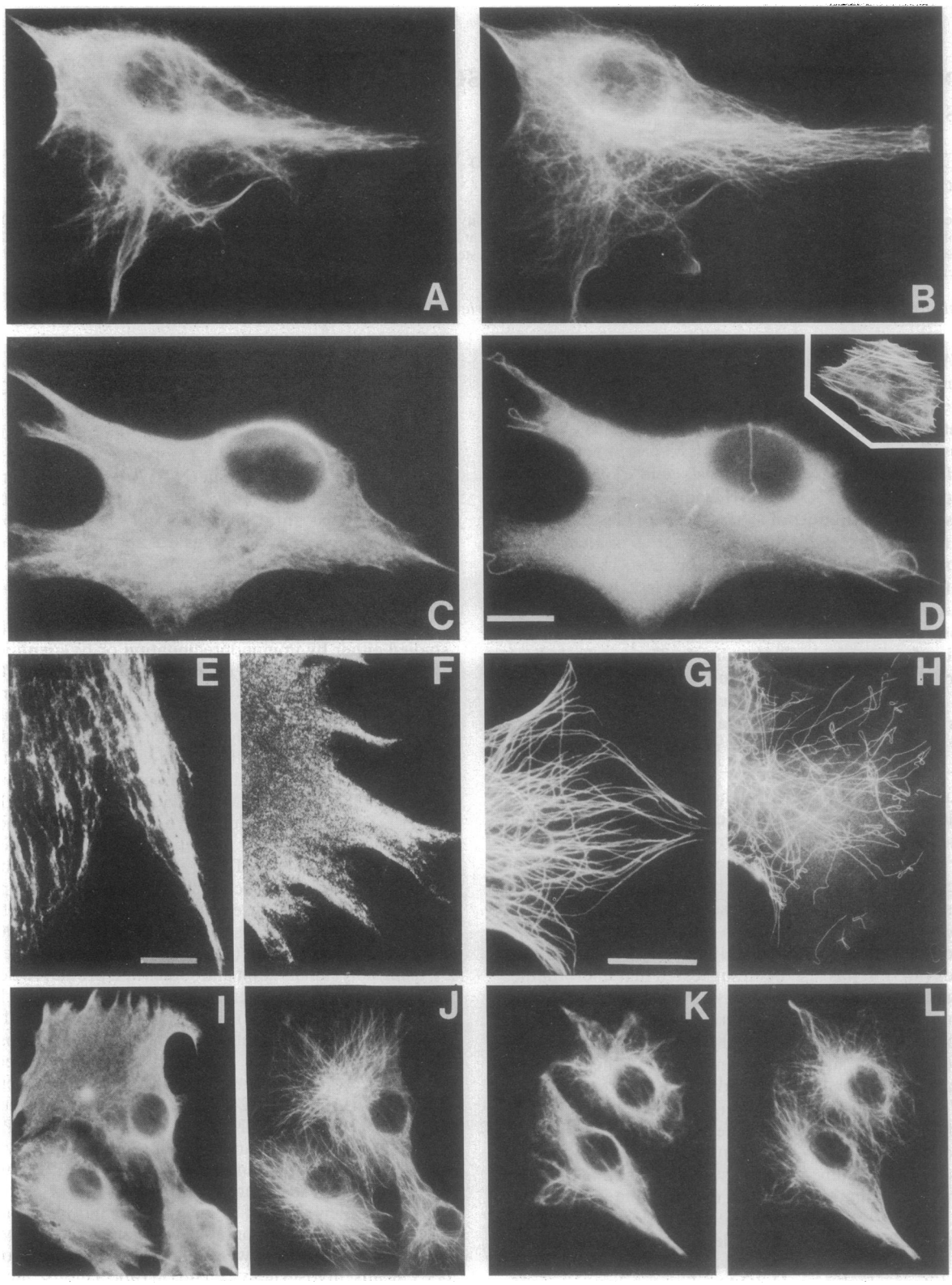

FIG. 1. Effects of phosphatase inhibitors on IFs and MTs in BHK-21 cells as determined by immunofluorescence. Photomicrographs show cells processed for double-label indirect immunofluorescence with a rabbit polyclonal antibody directed against vimentin and a mouse monoclonal antibody directed against β-tubulin. IF patterns are shown in *A*, *C*, *E*, *F*, *I*, and *K*. MT patterns are shown in *B*, *D*, *G*, *H*, *J*, and *L*. (*A* and *B*) Controls showing the normal distribution of IFs and MTs. The overall patterns of organization of these two cytoskeletal elements are similar due to the parallel arrangement of IFs and MTs in BHK-21 cells (21). (*C* and *D*) Typical cell 15–20 min after the addition of 20 nM cl-A. The overall vimentin pattern appears to be disrupted and diffuse and the tubulin antibody reveals only a few obvious MTs against a high background of diffuse fluorescence. (*D Inset*) Cell treated with 20 nM cl-A for 15 min, followed by fixation and staining with rhodamine-phalloidin. The actin-containing stress fibers revealed by this procedure appear normal. (*E–J*) Intermediate stages of IF and MT breakdown. (*E*) Confocal microscopic view of the peripheral region in a cell showing the details of a normal IF pattern. (*F*) Similar region in a cl-A-treated cell (20 nM, 5 min) viewed by confocal microscopy, revealing a much less filamentous more diffuse staining pattern, indicating that a significant change in IF structure has taken place. (*G*) Higher magnification view of a typical MT pattern in the peripheral region of an untreated cell. (*H*)

of $p34^{cdc2}$ phosphorylation sites (3), rounded-up mitotic cells were mechanically shaken off and discarded prior to cell lysis. For peptide mapping of the mitotic phosphorylation sites, cells were ^{32}P-labeled for 3 h in the presence of nocodazole (0.4 μg/ml; refs. 3 and 5). Cells arrested in mitosis were then mechanically shaken off, washed, and finally lysed in 0.4% SDS. Immunoprecipitation, tryptic digestion of vimentin, and two-dimensional thin-layer chromatography were performed as described (3–5).

RESULTS AND DISCUSSION

When BHK-21 cells were incubated with nanomolar to micromolar doses of cl-A, DT, or OA, normal IF structure was rapidly lost followed by a loss of MTs, as determined by indirect immunofluorescence (Fig. 1). A clear difference in the effective doses of cl-A, DT, and OA became apparent within 20 min of incubation. cl-A induced marked alterations in the cytoskeletal networks starting at a dose range of 10–20 nM, whereas 0.5–1 μM DT and 1–1.5 μM OA had to be used to induce similar effects. The hundredfold difference in inhibitor sensitivity is consistent with inhibition of PP1 being necessary to produce the effects.

Because cl-A was effective at much lower doses, it was used to examine the morphological effects in greater detail. Within 3–6 min, after the addition of 20 nM cl-A to intact cells, the vimentin IF networks appeared disrupted (Fig. 1). This was even more obvious after 9–10 min when an extensive loss of filamentous structures and the appearance of large areas of diffuse fluorescence was seen. At this same concentration, MT networks appeared normal for up to 5 min. However, by 9–10 min after cl-A addition, a noticeable reduction in the number of MT was observed in a large proportion of the cells, and at 15–20 min the bulk of the cells displayed only a small remaining proportion of MT. The decrease in the number of MTs was accompanied by a corresponding increase in diffuse fluorescence, indicating disassembly of MT networks. Furthermore, the MTs remaining after 15–20 min had a curly or kinky appearance that resembled the stable population of MTs (25). Although IFs and MTs were disorganized after 10–15 min in the presence of cl-A, cell shape was not obviously affected and the overall distribution and structure of actin-rich stress fibers (microfilament bundles) appeared normal, as determined by staining with rhodamine-labeled phalloidin (Fig. 1). After 20–30 min in the presence of 20 nM cl-A, an increasing number of the cells showed a more rounded morphology but still remained attached to the support. When cells rounded up, the organization of the stress fibers was altered (results not shown).

If these effects on IFs and MTs involve protein phosphorylation, they should be reversible. The normal morphological features of IF and MT networks were restored by allowing cells that had been treated for 20 min with 10–20 nM cl-A to recover for 2–6 h (10 nM, 2–4 h; 20 nM, 4–6 h) in normal medium (Fig. 1). This recovery demonstrates the continued viability of the cells and the reversibility of the cytoskeletal disruption induced by cl-A. The effects of OA and DT, at the relatively high doses required to mimic those of cl-A, were not reversible.

In accordance with previous studies on phosphatase inhibitors (see e.g., refs. 13–15, 26, and 27), cells incubated in the presence of cl-A, DT, or OA showed an overall increase in protein phosphorylation (Fig. 2). However, at low doses (20 nM) and short exposure times (5–20 min), when the effects on IFs and MTs were evident, only a few proteins showed

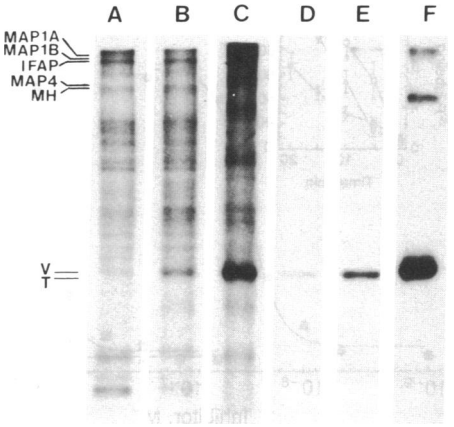

FIG. 2. Effects of cl-A on vimentin phosphorylation. Autoradiographs of ^{32}P-labeled proteins from whole cell lysates, separated by SDS/PAGE on a 7.5% gel. Lanes: A, control cells; B, cells incubated for 20 min in the presence of 20 nM cl-A; C, 50 nM cl-A. Immunoprecipitated vimentin was from the following cells. Lanes: D, control cells; E and F, cl-A-treated cells (20 and 50 nM, respectively, for 20 min). The positions of vimentin (V), myosin heavy chain (MH), MAP-4, IFAP-300 (IFAP), MAP-1A, and MAP-1B, respectively, are indicated. Of these proteins, at 10–20 nM cl-A, vimentin is the only protein to show a measurable increase in its phosphorylation state. The high molecular mass band in the autoradiograph on lane F is a small fraction of vimentin not fully dissociated from the antibody.

increased phosphorylation. The identity of the proteins that could be involved in the changes seen in IFs and MTs was further investigated. After 5–20 min of exposure to 10–20 nM cl-A, vimentin was the first protein showing measurable increases in ^{32}P labeling (Figs. 2 and 3). This was confirmed by immunoprecipitation (Fig. 2) and densitometric scans of autoradiographs of the immunoprecipitated vimentin (control, 0.11 AU; cl-A, 1.20 AU; cl-A/control, 10.9). The increases in vimentin phosphorylation corresponded well with the observed effects on IF network structure (Fig. 3). Immunoprecipitation of tubulin, MAP-1A, MAP-1B, and MAP-4 (MAPs known to be present in BHK-21 cells) revealed no changes in the ^{32}P labeling of these proteins after treatment with 20 nM cl-A for 20 min (control, 0.10, 0.07, 0.06, and 0.08 AU; cl-A, 0.09, 0.06, 0.06, and 0.09 AU; cl-A/control, 0.90, 0.86, 1.00, and 1.13, respectively). Likewise, immunoprecipitation of the IF crossbridging phosphoprotein IFAP-300K showed that the ^{32}P labeling of this protein remained unchanged (control, 0.21 AU; cl-A, 0.23 AU; cl-A/control, 1.10). Myosin heavy and light chains, shown to have increased phosphorylation levels in cl-A-treated 3T3 fibroblasts (14), were not affected under the conditions employed in the present study (control, 0.21 and 0.29 AU; cl-A, 0.22 and 0.32 AU; cl-A/control, 1.05 and 1.10, respectively). The discrepancy between these results and those of others is probably related to higher cl-A concentrations (10 times) and longer incubation times in the previous study (14).

There were obvious differences among the dose–response curves of cl-A, OA, and DT with respect to ^{32}P labeling of vimentin (Fig. 3). This corresponded to the observed differences in their effects on IF and MT networks. EC_{50} values for increased ^{32}P labeling of vimentin were as follows: cl-A, 27 nM; DT, 1100 nM; and OA, 1900 nM. The slight difference between the potencies of OA and DT is consistent with

Details of the MT pattern in a peripheral region of a cell after 10 min in 20 nM cl-A. At this stage there is a marked overall reduction in the MTs before the entire normal MT pattern is disrupted. Many of the MTs remaining appear to be kinked or curly. (*I* and *J*) Cells incubated 5 min in the presence of 20 nM cl-A. The vimentin staining is more diffuse and MTs appear normal, indicating that the IF networks are affected before the MTs. (*K* and *L*) Cells treated for 20 min with 20 nM cl-A, followed by washing and incubation in cl-A-free medium for 4 h. Both the IF and MT patterns appear normal. [Bars: *D*, 5 μm (applies for *A–D*); *E*, 1 μm (applies for *E* and *F*); *G*, 4 μm (applies for *G* and *H*).]

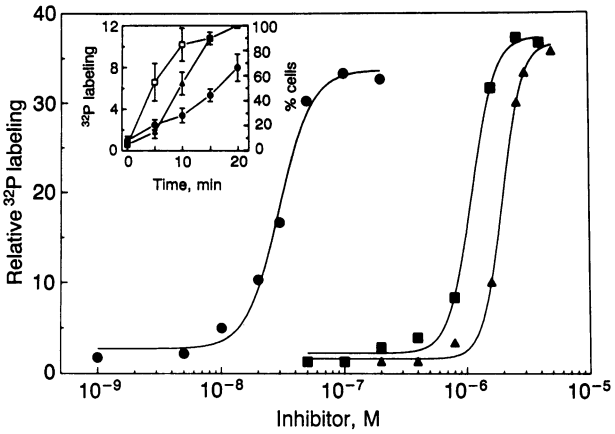

FIG. 3. Dose–response curves of cl-A (●), DT (■), and OA (▲) as measured by increases in vimentin ^{32}P labeling in BHK-21 cells. ^{32}P-labeled whole cell extracts were separated by SDS/PAGE on 7.5% gels and the relative increases in ^{32}P labeling (control = 1) were determined as absorbance units (AU) from densitometric scans of vimentin bands on autoradiographs or by β-scanner measurements of the radioactivity in vimentin bands on the dried gels. Similar results were obtained by both methods. The differences among the potencies of cl-A vs. DT or OA suggest that PP1 rather than PP2A is involved in the observed effects. Notice that some of the data points are overlapping and may thus appear to be missing. (*Inset*) Time-course increase of the ^{32}P labeling of vimentin (●) from cells incubated in the presence of 20 nM cl-A (measurements were carried out as described above). The increases in ^{32}P labeling were correlated with the alterations in the morphology of IFs and MTs. The percentage of cells displaying IF (□) and MT (△) morphologies corresponding to those shown in Fig. 1 *C*, *D*, *H*, and *I* were counted as altered. Numbers indicate the mean ± range of values. These observations were carried out independently by three persons in the laboratory, with similar results.

previous observations on the relative inhibitory activities of these compounds against PP1 and PP2A (19, 27).

Although cl-A is a highly specific phosphatase inhibitor that does not act directly upon any of the kinases examined to date (15), it could have indirect effects. For example, it has been suggested that OA, when the conditions are favorable, as in G_2 (28) and S (29) phases, can induce activation of $p34^{cdc2}$ kinase. However, in the present study, the enhanced phosphorylation of vimentin in response to cl-A occurred at sites in the protein that were normally phosphorylated in interphase cells. This was demonstrated by two-dimensional phosphopeptide mapping of vimentin immunoprecipitated from control cells, cl-A-treated cells, and mitotic cells (Fig. 4). The results showed that the vimentin phosphopeptide maps from both control cells and cl-A-treated cells had virtually identical patterns (i.e., the same number of phosphopeptides at the same relative positions). A quantification of the ^{32}P labeling, however, revealed that vimentin peptide maps from cl-A-treated cells showed a marked fold increase of ^{32}P labeling of two sites, peptides b and c (22 ± 6 and 45 ± 15, respectively; mean ± range; $N = 3$), and overall increases at all sites (<10-fold) except one (peptide a; Fig. 4). The same sites showed increased ^{32}P labeling in vimentin from cl-A-treated cell cultures synchronized in G_1 phase (J.E.E. and R.D.G., unpublished results). In comparison, mitotic vimentin peptide maps revealed that none of these sites corresponded to the mitotic phosphorylation sites specific for $p34^{cdc2}$ kinase (peptide a) and vimentin kinase I (peptides i and j; refs. 3–5). Since mitotic vimentin kinase sites did not show any increases in ^{32}P labeling upon cl-A treatment, cl-A evidently does not induce vimentin kinase activities other than those already active in interphase cells. The interphase sites (peptides b and c) displaying the most obvious increases in ^{32}P labeling could be preferential vimentin dephosphorylation sites for serine/threonine protein phosphatases.

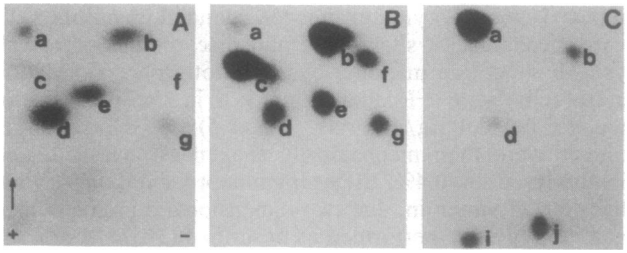

FIG. 4. Tryptic [^{32}P]phosphopeptide maps of vimentin immunoprecipitated from BHK-21 fibroblasts demonstrate that inhibition of protein phosphatases with cl-A does not activate kinases other than those already active in interphase cells. The phosphopeptide maps derived from vimentin of control cells (*A*) and cl-A-treated cells (*B*) show identical patterns [i.e., the same number of peptides at the same relative positions, although some of the phosphopeptides show markedly increased labeling (see below)]. The identical patterns in both preparations suggest that only interphase kinases are active in both preparations. In contrast, the peptide map of vimentin derived from cells blocked in mitosis by nocodazole treatment is completely different (*C*). This map shows the characteristic phosphorylation sites of the mitotic kinases $p34^{cdc2}$ (peptide a; see refs. 3 and 4 for further details) and vimentin kinase I (peptides i and j, respectively, see refs. 3 and 5 for further details). Measurements of the ^{32}P labeling on the maps, as determined with a β-scanner, revealed that there are no significant relative increases on the mitotic sites (peptides a, i, and j) in vimentin peptide maps from cl-A-treated interphase cells. In contrast, all of the phosphopeptides, except peptide a, seen in the map obtained from control cells showed overall increases in the ^{32}P labeling (see text for details). Combinations of the different samples were electrophoresed to confirm the identity of individual peptides (results not shown). Peptides that were not detectable on the autoradiographs of the respective maps have not been lettered. Directions of electrophoresis (+ and −) and ascending chromatography (arrow) are indicated.

Both of the predominant protein phosphatases in animal cells, PP1 and PP2A, are inhibited by approximately the same nanomolar concentrations of cl-A (15, 27). On the other hand, OA discriminates between the two phosphatases, inhibiting PP2A at 50- to 100-fold lower concentrations than those effective for PP1. Our results, showing that 50- to 100-fold higher concentrations of DT and OA are required to produce effects similar to those of cl-A on IF and MT organization and vimentin phosphorylation, are consistent with an inhibition of PP1 being necessary to produce the effects. Evidence in support of a role for PP1 in the regulation of IF organization and vimentin phosphorylation has also been derived from the microinjection of purified PP1 into fibroblasts, resulting in both the stabilization of IFs during heat shock and the induction of lower levels of ^{32}P labeling of vimentin (30).

The results of this study have led us to conclude that protein phosphatase activity is involved in the maintenance of the structural integrity of cytoskeletal IF networks. This conclusion is based on the very rapid increase of vimentin phosphorylation and the corresponding alterations in IF structure seen by immunofluorescence that accompany the treatment of BHK-21 cells with the phosphatase inhibitor cl-A. In further support of these observations, it has been shown that increased phosphorylation of IF proteins *in vitro* and *in vivo* leads to their disassembly (2). The rapid structural alterations in IF networks induced by cl-A treatment seem to be followed by MT disruption at slightly later times. Several studies have shown that IFs and MTs are closely associated with each other both spatially and presumably functionally, by largely unknown mechanisms (21, 31, 32). Our results indicate an initial disruption of vimentin IF networks with subsequent effects on MT networks. This observation further emphasizes the close association between these two cytoskeletal systems. Although it is apparent that the cl-A-induced increase in vimentin phosphorylation affects IF structure, it is still unclear how this

relates to the observed effects on MT organization and structure. Since there are not obvious alterations in the phosphorylation states of either tubulin or MAPs, it seems unlikely that there is a direct effect of phosphatase inhibition on any of the major MT structural proteins or MAPs. However, it is plausible that there could be phosphorylation-dependent effects on some unidentified minor MT-severing protein, as suggested (9). Furthermore, our results are consistent with observations indicating that OA can interfere with MT dynamics (33). Thus these data suggest that protein phosphatases, especially of PP1-type, are of critical importance in maintaining the normal interphase structure of two major cytoskeletal systems in mammalian cells. Previous studies have indicated that protein phosphatases are important in regulating other cytoskeletal proteins, such as the actomyosin complex (12–14). However, in the present study, during the time course when the cl-A-induced effects on IFs and MTs occurred, both morphology and phosphorylation of the actomyosin system remained unchanged. This may indicate that this latter system is affected at another level of overall protein phosphorylation in cells.

Vimentin shows a low degree of phosphorylation in interphase cells despite the presence of many potential phosphorylation sites (4). Our results showing rapid increases in vimentin phosphorylation in cells treated with cl-A indicate that this is probably a consequence of a high protein phosphatase activity, rather than low constitutive activities of kinases acting on vimentin. In addition, this observation points to a high turnover rate of phosphate on vimentin. The purpose of this high turnover rate may be related to the regulation of IF assembly states *in vivo*. For example, the finding that the soluble or unpolymerized pool of vimentin subunits in interphase cells is small (1, 2) may be due to protein phosphatase activity maintaining low levels of phosphorylated vimentin. This would favor the polymerized form of vimentin during interphase. In contrast, vimentin has been shown to disassemble upon elevated phosphorylation in some type of cells in mitosis (3, 5). Therefore, the high constitutive vimentin phosphatase activity, inferred from our studies, may be involved in maintaining IFs in the assembled form in interphase cells. When the kinase–phosphatase equilibrium is altered, as in mitosis, the consequent elevation of vimentin phosphorylation would favor disassembly (3, 5). In further support of this, there is evidence for a cell-cycle-dependent cytoskeletal translocation of PP1 (34) that may allow phosphorylation of selected cellular components, such as nuclear lamins (35) and vimentin (3–5) by $p34^{cdc2}$ during mitosis. The two preferential dephosphorylation sites in normal interphase cells, as indicated by the peptide maps, may be especially important in the regulation of vimentin dynamics. Regulation of the phosphorylation states of vimentin and perhaps keratin may also underlie the mechanisms involved in the exchange between IF protein subunits and polymers recently elucidated by studies employing microinjection and fluorescence recovery after photobleaching (36, 37). It is noteworthy that the reversible effects of cl-A on IF structure should make it useful for *in vivo* studies on the role of phosphorylation in IF assembly and function. Overall, the data available support the intriguing idea that an orchestrated activation and deactivation of protein phosphatases and kinases, such as PP1 and $p34^{cdc2}$, could account for the dynamic properties of IFs seen during different phases of the cell cycle.

We thank Satya Khuon and Michelle Lowy for skillful technical assistance. J.E.E. is supported by a Fogarty International Fellowship from the National Institutes of Health and by the Academy of Finland. R.D.G. is supported by National Institutes of Health Grant GM 36806.

1. Skalli, O. & Goldman, R. D. (1991) *Cell Motil. Cytoskeleton* **19**, 67–69.
2. Eriksson, J. E., Opal, P. & Goldman, R. D. (1992) *Curr. Opin. Cell Biol.* **4**, 99–104.
3. Chou, Y.-H., Bischoff, J. R., Beach, D. & Goldman, R. D. (1990) *Cell* **62**, 1063–1071.
4. Chou, Y.-H., Ngai, K.-L. & Goldman, R. D. (1991) *J. Biol. Chem.* **266**, 7325–7328.
5. Chou, Y.-H., Rosevear, E. & Goldman, R. D. (1989) *Proc. Natl. Acad. Sci. USA* **86**, 1885–1889.
6. Bershadsky, A. D. & Gelfand, V. I. (1981) *Proc. Natl. Acad. Sci. USA* **78**, 3610–3613.
7. Therkauf, W. E. & Vallee, R. B. (1982) *J. Biol. Chem.* **257**, 3284–3290.
8. Olmstedt, J. (1991) *Curr. Opin. Cell Biol.* **3**, 52–58.
9. Vale, R. D. (1991) *Cell* **64**, 827–839.
10. Yamashira, S. & Matsumura, F. (1991) *BioEssays* **13**, 563–568.
11. Sellers, J. R. (1991) *Curr. Opin. Cell Biol.* **3**, 98–104.
12. Fernandez, A., Brautigan, D. L., Mumby, M. & Lamb, N. J. C. (1990) *J. Cell Biol.* **111**, 103–112.
13. Eriksson, J. E., Toivola, D., Meriluoto, J. A. O., Karaki, H., Han, Y.-G. & Hartshorne, D. (1990) *Biochem. Biophys. Res. Commun.* **173**, 1347–1353.
14. Chartier, L., Rankin, L. L., Allen, E. R., Kato, Y., Fusetani, N., Karaki, H., Watabe, S. & Hartshorne, D. J. (1991) *Cell Motil. Cytoskeleton* **18**, 26–40.
15. Cohen, P., Holmes, C. F. B. & Tsukitani, Y. (1990) *Trends Biochem. Sci.* **15**, 98–102.
16. Yang, Y.-H., Lieska, N., Goldman, A. & Goldman, R. D. (1985) *J. Cell Biol.* **100**, 620–631.
17. Starger, J., Brown, W. E., Goldman, A. & Goldman, R. D. (1978) *J. Cell Biol.* **78**, 93–109.
18. Eriksson, J. E., Paatero, G. I. L., Meriluoto, J. A. O., Codd, G. A., Kass, G. E. N., Nicotera, P. & Orrenius, S. (1989) *Exp. Cell Res.* **185**, 86–100.
19. Fujiki, H., Suganuma, M., Suori, I., Yoshizava, S., Tagaki, K., Uda, N., Wakamatsu, K., Yamada, K., Murata, M., Yasumoto, T. & Sugimura, T. (1988) *Jpn. J. Cancer Res.* **79**, 1089–1093.
20. Parysek, L. M., Esnes, C. S. & Olmsted, J. B. (1984) *J. Cell Biol.* **99**, 1309–1315.
21. Wang, E. & Goldman, R. D. (1978) *J. Cell Biol.* **79**, 708–726.
22. Bloom, G. S., Schoenfeld, T. & Vallee, R. B. (1984) *J. Cell Biol.* **98**, 320–330.
23. Bloom, G. S., Luca, F. C. & Vallee, R. B. (1985) *Proc. Natl. Acad. Sci. USA* **82**, 5404–5408.
24. Laemmli, U. K. (1970) *Nature (London)* **227**, 680–685.
25. Gundersen, G. G., Kalinoski, M. H. & Bulinsk, J. C. (1984) *Cell* **38**, 779–789.
26. Yatsunami, J., Fujiki, H., Suganuma, M., Yoshizava, S., Eriksson, J. E., Olson, M. O. J. & Goldman, R. D. (1991) *Biochem. Biophys. Res. Commun.* **177**, 1165–1169.
27. Ishihara, H., Martin, B. L., Brautigan, D. L., Karaki, H., Ozaki, H., Kato, Y., Fusetani, N., Watabe, S., Hashimoto, K., Uemura, D. & Hartshorne, D. J. (1989) *Biochem. Biophys. Res. Commun.* **159**, 871–877.
28. Picard, A., Labbe, J. C., Barakat, H., Cavadore, J. C. & Doree, M. (1991) *J. Cell Biol.* **115**, 337–344.
29. Yamashita, K., Yasuda, H., Pines, J., Yasumoto, K., Nishitani, H., Ohtsubo, M., Hunter, T., Sugimura, T. & Nishimoto, T. (1991) *EMBO J.* **9**, 4331–4338.
30. Brautigan, D. L., Fernandez, A. & Lamb, N. J. C. (1989) *Adv. Protein Phosphatases* **5**, 547–566.
31. Blose, S. H., Meltzer, D. I. & Feramisco, J. R. (1984) *J. Cell Biol.* **98**, 847–858.
32. Gyoeve, F. K. & Gelfand, V. I. (1991) *Nature (London)* **353**, 445–448.
33. Vandré, D. D. & Wills, V. L. (1992) *J. Cell Sci.* **101**, 79–91.
34. Fernandez, A., Brautigan, D. L. & Lamb, N. (1992) *J. Cell Biol.* **116**, 1421–1430.
35. Peter, M., Nagakawa, J., Dorée, M., Labbe, J. C. & Nigg, E. A. (1990) *Cell* **61**, 591–602.
36. Miller, R., Vikstrom, K. & Goldman, R. D. (1991) *J. Cell Biol.* **113**, 843–855.
37. Vikstrom, K., Lim, S.-S., Goldman, R. D. & Borisy, G. G. (1992) *J. Cell Biol.* **118**, 121–129.